

NOTICE: Ukraine: Read IOP Publishing’s statement.

Table of contents

Volume 963

2022

◀ Previous issue Next issue ▶

International Bioprocessing Association Subject Conference (IBASC 2021) 4th-5th August 2021, Yogyakarta, Indonesia

Accepted papers received: 20 December 2021

Published online: 19 January 2022

Open all abstracts

Preface

OPEN ACCESS	011001
Preface – International Bioprocessing Association Subject Conference (IBASC 2021)	
+ Open abstract View article PDF	

OPEN ACCESS	011002
Peer review declaration	
+ Open abstract View article PDF	

Bioenergy/biofuel

OPEN ACCESS	012001
Performance evaluation of four-wheel driving wheel tractor with diesel engine using biodiesel fuel	
D A Sasmito, L T Mulyantara and A Budiman	
+ Open abstract View article PDF	

OPEN ACCESS	012002
Synthesis of zeolite catalyst for palm oil cracking process by means of microwave induced local kaolin leaching	
S Shoelarta, A F Haryati and D R Suminar	
+ Open abstract View article PDF	

OPEN ACCESS	012003
Process design and simulation of industrial-scale biodiesel purification using membrane technology	
S P Kusumocahyo, R C Redulla, K Fulbert and A A Iskandar	
+ Open abstract View article PDF	

OPEN ACCESS	012004
Advance of glucose conversion to 5-hydroxymethylfurfural using ionic liquid: mini review	
M Zunita, D M Yus and A S Leksone	
+ Open abstract View article PDF	



OPEN ACCESS	012005
Impact of surfactant-aided subcritical water pretreatment process conditions on the reducing sugar production from oil palm empty fruit bunch	
A N L Rachmah, A Fatmawati and A Widjaja	
<div><div><div><div></div></div><div>Open abstract</div></div><div><div><div></div></div><div>View article</div></div><div><div><div></div></div><div>PDF</div></div></div>	
OPEN ACCESS	012006
Analysis of biogas production from palm oil mill effluent at different feed flow rates in biogas plant Sei Pagar Riau	
W Wulandari and S P Senda	
<div><div><div><div></div></div><div>Open abstract</div></div><div><div><div></div></div><div>View article</div></div><div><div><div></div></div><div>PDF</div></div></div>	
OPEN ACCESS	012007
Potential of biomass and coal co-firing power plants in Indonesia: a PESTEL analysis	
A Sugiyono, I Febijanto, E Hilmawan and Adiarso	
<div><div><div><div></div></div><div>Open abstract</div></div><div><div><div></div></div><div>View article</div></div><div><div><div></div></div><div>PDF</div></div></div>	
OPEN ACCESS	012008
Effect of CaO/SiO ₂ compositions on the structure formation of mesoporous calcium silicate (CaSiO ₃) composite particles as adsorbent for organic dye removal	
L Ernawati, A W Yusariarta, R Alviany and A Halim	
<div><div><div><div></div></div><div>Open abstract</div></div><div><div><div></div></div><div>View article</div></div><div><div><div></div></div><div>PDF</div></div></div>	
OPEN ACCESS	012009
Influence of fenton pretreatment on anaerobic digestion of sugarcane vinasse: effect of H ₂ O ₂ dosage	
D C Hakika, S Sarto, A Mindaryani and M Hidayat	
<div><div><div><div></div></div><div>Open abstract</div></div><div><div><div></div></div><div>View article</div></div><div><div><div></div></div><div>PDF</div></div></div>	
OPEN ACCESS	012010
Thermogravimetric analysis kinetic study of <i>Spirulina platensis</i> residue pyrolysis	
S Jamilatun, A Aktawan, A Budiman and I Mufandi	
<div><div><div><div></div></div><div>Open abstract</div></div><div><div><div></div></div><div>View article</div></div><div><div><div></div></div><div>PDF</div></div></div>	
OPEN ACCESS	012011
Energy balance analysis on increasing the capacity of a sugar factory in Indonesia	
A Wibowo	
<div><div><div><div></div></div><div>Open abstract</div></div><div><div><div></div></div><div>View article</div></div><div><div><div></div></div><div>PDF</div></div></div>	
OPEN ACCESS	012012
Copyrolysis of rice husk and plastic bags waste from low-density polyethylene (LDPE) for improving pyrolysis liquid product	
H Wijayanti, C Irawan and N Aulia	
<div><div><div><div></div></div><div>Open abstract</div></div><div><div><div></div></div><div>View article</div></div><div><div><div></div></div><div>PDF</div></div></div>	
OPEN ACCESS	012013
Modeling the synthetic gas fermentation for bioethanol production	
G M Krista and M T A P Kresnowati	
<div><div><div><div></div></div><div>Open abstract</div></div><div><div><div></div></div><div>View article</div></div><div><div><div></div></div><div>PDF</div></div></div>	



OPEN ACCESS	012014
A review of sugarcane bagasse pretreatment for bioethanol production	
M H Nasution, S Lelinasari and M G S Kelana	
<div><div><div><div></div></div><div>Open abstract</div></div><div><div><div></div></div><div>View article</div></div><div><div><div></div></div><div>PDF</div></div></div>	
OPEN ACCESS	012015
Growth rate measurements of <i>Chlorella vulgaris</i> in a photobioreactor by Neubauer-improved counting chamber and densitometer	
S Ma'mun, A Wahyudi and A S Raghdanesa	
<div><div><div><div></div></div><div>Open abstract</div></div><div><div><div></div></div><div>View article</div></div><div><div><div></div></div><div>PDF</div></div></div>	
OPEN ACCESS	012016
Myco-briquettes from sugar palm dregs fibre, cassava dregs and coconut shell charcoal with solid substrate fermentation technology	
W Agustina, P Aditiawati and S S Kusumah	
<div><div><div><div></div></div><div>Open abstract</div></div><div><div><div></div></div><div>View article</div></div><div><div><div></div></div><div>PDF</div></div></div>	
OPEN ACCESS	012017
Development of lignocellulose-based bioethanol from chrysanthemum flower waste (<i>Chrysanthemum sp.</i>)	
A D Nugrahini, M P Kurniawan and D A Kinasih	
<div><div><div><div></div></div><div>Open abstract</div></div><div><div><div></div></div><div>View article</div></div><div><div><div></div></div><div>PDF</div></div></div>	
OPEN ACCESS	012018
Hydrodynamic study of internal circulation inside microreactor for transesterification process	
V R a/l S Rae, A M Laziz and K Z K Shaari	
<div><div><div><div></div></div><div>Open abstract</div></div><div><div><div></div></div><div>View article</div></div><div><div><div></div></div><div>PDF</div></div></div>	
Biomaterial engineering	
OPEN ACCESS	012019
Effect of solid loading and dipping time on microstructure and shear strength of hydroxyapatite coatings deposited via dip coating technique	
A Fadli, N Mulya, K B Pane and A Pratama	
<div><div><div><div></div></div><div>Open abstract</div></div><div><div><div></div></div><div>View article</div></div><div><div><div></div></div><div>PDF</div></div></div>	
OPEN ACCESS	012020
The effect of surfactant on the hydrolysis of coconut husk using cellulase and xylanase enzyme immobilized on chitosan magnetic nanoparticles	
C Tiatira, A Hamzah, H F Sangian and A Widjaja	
<div><div><div><div></div></div><div>Open abstract</div></div><div><div><div></div></div><div>View article</div></div><div><div><div></div></div><div>PDF</div></div></div>	
OPEN ACCESS	012021
Production of bone implant filaments from blue crab shells (<i>Portunus pelagicus</i>) in various synthesis conditions and blending ratios of hydroxyapatite (HAp)-polycaprolactone (PCL)	
E O Ningrum, E L Pratiwi, I L Shaffitri, A F P Putra, A D Karisma and S Suprpto	
<div><div><div><div></div></div><div>Open abstract</div></div><div><div><div></div></div><div>View article</div></div><div><div><div></div></div><div>PDF</div></div></div>	
OPEN ACCESS	012022
This site uses cookies. By continuing to use this site you agree to our use of cookies. To find out more, see our Privacy and Cookies policy.	

A mini-review of bio-scrubber derived from bacterial cellulose impregnated by flavonoid of moringa leaves

A N Sa’adah, G N A Milyawan, T Nadya and S Silviana

[+ Open abstract](#) [View article](#) [PDF](#)

OPEN ACCESS 012023

Superhydrophobic coating based on silica derived from bagasse modified with vinyltriethoxysilane and copper (Cu) as antibacterial agent

S Silviana, A N Sa’adah, K B Saputra, B E Naftalina, C R Kroon, G N Catherine, L Subianto, M E Annisa, R U Maghfira, T D Azzahra *et al*

[+ Open abstract](#) [View article](#) [PDF](#)

OPEN ACCESS 012024

Synthesis and characterization of cellulose-based graft copolymers crosslinked by gamma-irradiation for enhanced oil recovery applications

A Z Abidin, R P Putra, B F Aulia, F Kurniangga and G I Fajar

[+ Open abstract](#) [View article](#) [PDF](#)

OPEN ACCESS 012025

Fabrication and characterization of FITC-modified naturalbased silica nanoparticles using sol-gel method

N O Sifana and S N A Jenie

[+ Open abstract](#) [View article](#) [PDF](#)

OPEN ACCESS 012026

The rheological and mechanical properties of natural rubber/graphene composites

P Marlina, H A Prasetya, Rahmaniar, Nasruddin, A K Nugroho, M K Yusya, R Andika and S Haryati

[+ Open abstract](#) [View article](#) [PDF](#)

OPEN ACCESS 012027

Synthesis of silica-cellulose aerogel derived from bagasse through impregnation and ambient pressure drying methods as thermal insulator

S Silviana, A N Sa’adah, R P Deastuti, N C Ramadhani, N Simarmata, L E Arianto, M Y Tiurma, J Rahmaningrum, F Fauzi and M A S Mahmud

[+ Open abstract](#) [View article](#) [PDF](#)

OPEN ACCESS 012028

Synthesis of palm oil-base zinc stearate and its application on manufacture of rubber component

W B Setianto, H Yohanes, Astuti, Maisaroh and G Atmaji

[+ Open abstract](#) [View article](#) [PDF](#)

OPEN ACCESS 012029

Effect carbon black and modified kaolin hybrid filler on the curing and physic-mechanical properties of natural rubber-styrene butadiene rubber blends

T Susanto, Rahmaniar, V. G. V Putra, T I Sari, Farida, K A Roni and G Puspitasari

[+ Open abstract](#) [View article](#) [PDF](#)

OPEN ACCESS 012030

The effect of silica filler quartz sand from tailing processing of mining material on mechanical properties, thermal aging and morphology rubber compound

This site uses cookies. By continuing to use this site you agree to our use of cookies. To find out more, see our Privacy and Cookies policy.



H A Prasetya, P Marlina, Rahmaniar, B Sugiyono, F Danimasthari, Subari and M Faizal

 Open abstract

 View article

 PDF

OPEN ACCESS012031

Preparation of magnesium oxide confined in activated carbon synthesized from palm kernel shell and its application for hydrogen sulfide removal

D Abriyani, T Ariyanto and I Prasetyo

 Open abstract

 View article

 PDF

OPEN ACCESS012032

Studies on the curing, tensile and adhesion characteristics of cushion gum to carcass in truck retreaded tires: the effect natural rubber types

Rahmaniar, T Susanto, P Marlina, H A Prasetya and M Purbaya

 Open abstract

 View article

 PDF

OPEN ACCESS012033

Functionalization of multi-walled carbon nanotube (MWCNT) with CTACe surfactant and polyethylene glycol as potential drug carrier

S D Primastari, Y Kusumastuti, M Handayani and Rochmadi

 Open abstract

 View article

 PDF

Environmental biotechnology

OPEN ACCESS012034

High cell density submerged membrane photobioreactor (SMPBR) for microalgae cultivation

S Steven, D L Friatnasary, A K Wardani, K Khoiruddin, G Suantika and I G Wenten

 Open abstract

 View article

 PDF

OPEN ACCESS012035

The effect of temperatures and monomer ratios on the characteristic of anionic and cationic gel-based adsorbents

E O Ningrum, Z M Safitri, M A Dzaky, S Suprpto, A D Karisma and H Ni'mah

 Open abstract

 View article

 PDF

OPEN ACCESS012036

The role of C/N ratio on anaerobic decomposition of industrial tempeh wastewater for optimizing methane production

Y Fransiscus and T L Simangunsong

 Open abstract

 View article

 PDF

OPEN ACCESS012037

Biomethanization technology application on slaughterhouse in Indonesia

N Ginting

 Open abstract


 View article


 PDF


OPEN ACCESS012038

Nitrate (NO³⁻) removal from wastewater by adsorption using modified kaolin


L H Lubis, A Husin and Z Masyitah

 Open abstract

 View article

 PDF

This site uses cookies. By continuing to use this site, you agree to our use of cookies. To find out more, see our Privacy and Cookies policy.




OPEN ACCESS012039


The effect of pH, initial concentration, and salinity on the biosorption process of chromium (VI) ions using microalgae *Chlorella sp.*

K C Wanta, D Saptoaji, Y I P A Miryanti and A P Kristijarti

+

Open abstract

View article

PDF


OPEN ACCESS012040


Comparison of different phytoremediation strategies for acid mine drainage (AMD)

R A Rahman, J Wintoko and A Prasetya

+

Open abstract

View article

PDF


OPEN ACCESS012041


Potential of natural sunlight for microalgae cultivation in Yogyakarta

E Habibah, E A Suyono, M D Koerniawan, L T Suwanti, U J Siregar and A Budiman

+

Open abstract

View article

PDF

Food technology/engineering


OPEN ACCESS012042


The extraction and purification of squalene from Nyamplung (*Calophyllum Inophyllum L*) leaves

D H Ardhyini, H W Aparamarta, A Widjaja, R Ibrahim and S Gunawan

+

Open abstract

View article

PDF


OPEN ACCESS012043


Separation of proanthocyanidin from red sorghum seed extract using macroporous resin

M Musdzalifah, M Fahrurrozi, W B Sediawan and D Y Susanti

+

Open abstract

View article

PDF

Industrial biotechnology


OPEN ACCESS012044


Computational study of the acetic acid extraction process from an aqueous solution with the aid of biological buffer

S Altway, N B Ramli, M I Maulidia, S Soeprijanto, D R Zuchrillah and A H Tiwikrama

+

Open abstract

View article

PDF


OPEN ACCESS012045


Removal of ammonia in raw water taken from Surabaya river using biofiltration process

N I Said, W Widayat, S Yudo, M A Kholiq and Setiyono

+

Open abstract

View article

PDF


OPEN ACCESS012046


Economic analysis on the potential of palm oil empty fruit bunch pellets as alternative fuel to reduce the cost of the government’s 3 kg LPG subsidy and its role in achieving sustainable development goals

L A Dewanjaya, A T Yuliansyah and E A Suyono

+

Open abstract

View article


PDF


OPEN ACCESS012047

The effect of ultrasonic extraction methods on extract quality from *Strobilanthes crispus* L.

R Arbianti, H Ningsih, T S Utami, Y Muharam and Slamet

+ Open abstract

 View article


 PDF


OPEN ACCESS012048

Modeling of extraction of silica rendemen husk rice (*Oryza sativa* L.) by microwave extraction assisted (MAE) using response surface methodology (RSM)

D W Indriani and T R Wardhani

+ Open abstract

 View article


 PDF


OPEN ACCESS012049

Evaluation of volatile fatty acids (VFAs) production in thermophilic and mesophilic anaerobic digestion of oil palm empty fruit bunch (OPEFB)

A Sanjaya, K Mondylaksita, R Millati and W Budhijanto

+ Open abstract

 View article

 PDF


Waste to Resources


OPEN ACCESS012050

Simple mass transfer simulation using a single-particle heterogeneous reaction approach in rice husk combustion and rice husk ash extraction

S Steven, E Restiawaty and Y Bindar

+ Open abstract

 View article


 PDF


OPEN ACCESS012051

Study of domestic wastewater in oil and gas field: A case study in the Cangkring river, Tuban, East Java

A S Patimah, A Prasetya and S H Murti

+ Open abstract

 View article


 PDF


OPEN ACCESS012052

Synthesis and pot trial of organic fertilizer from solid waste

C W Purnomo, P Noviyani, S Indarti and G T Schriefer

+ Open abstract

 View article


 PDF


OPEN ACCESS012053

Glucose production from oil palm empty fruit bunch (OPEFB) using microwave and fungal treatment method

S R Juliastuti, N Hendrianie, K R Sabar and S Anggita

+ Open abstract

 View article


 PDF


OPEN ACCESS012054

Characteristic of oil palm empty fruit bunch after ethanol-organosolv pretreatment catalyzed by acid

K Mondylaksita, W Budhijanto, M J Taherzadeh and R Millati

+ Open abstract

 View article

 PDF

OPEN ACCESS012055

Microcrystalline cellulose production by acid hydrolysis of hydroponic rice straw pulp

R Raudiana Syarifan, W B Sedawan, M M Azis and I Hartati

Open abstract

View article

PDF

OPEN ACCESS

012056

Batch electrocoagulation system using aluminum and stainless steel 316 plates for hospital wastewater treatment

R Muttaqin, R Ratnawati and S Slamet

Open abstract

View article

PDF

OPEN ACCESS

012057

Subsurface flow constructed wetland model for phytoremediation of chromium from tannery wastewater using *Echinodorus palaefolius*

L Prasakti, D Melyta, Sarto and A Prasetya

Open abstract

View article

PDF

OPEN ACCESS

012058

Utilization of sodium silica from coal fly ash and trimethylchlorosilane as self-cleaning coating on glass

I K Maharsih, L Ernawati, Welltina and W P Dani

Open abstract

View article

PDF

OPEN ACCESS

012059

Utilization of gambier leaf extract (*Uncaria gambier roxb*) as antibacterial and natural dyes in making liquid bath soap with natrium lauryl ether sulfate

C Nurhayati, N Susilawati, T Susanto, W Marthalia and A K Nugroho

Open abstract

View article

PDF

JOURNAL LINKS

Journal home

Journal scope

Information for organizers

Information for authors

Contact us

Reprint services from Curran Associates



PAPER • OPEN ACCESS

Thermogravimetric analysis kinetic study of *Spirulina platensis* residue pyrolysis

To cite this article: S Jamilatun *et al* 2022 *IOP Conf. Ser.: Earth Environ. Sci.* **963** 012010

View the [article online](#) for updates and enhancements.

You may also like

- [Response of *Spirulina Platensis* to Sulfamethazine Contamination](#)
Xiankuan Xu, Xiaohong Lu, Xiangjuan Ma et al.
- [Growth of Microalgae *Spirulina platensis* on Media Containing Palm Oil Mill Effluent](#)
I. Effendi, I. Nurrachmi and A. N. F. Tarigan
- [Modification of Microencapsulate Protein Crude Extract Formula from *Chlorella vulgaris* and *Spirulina platensis* for Baby Biscuit](#)
E Mayasari, I Raya, Z Dwyana et al.



*Benefit from connecting
with your community*

ECS Membership = Connection

ECS membership connects you to the electrochemical community:

- Facilitate your research and discovery through ECS meetings which convene scientists from around the world;
- Access professional support through your lifetime career;
- Open up mentorship opportunities across the stages of your career;
- Build relationships that nurture partnership, teamwork—and success!

Join ECS!

Visit electrochem.org/join



Thermogravimetric analysis kinetic study of *Spirulina platensis* residue pyrolysis

S Jamilatun^{1*}, A Aktawan¹, A Budiman², I Mufandi³

¹Department of Chemical Engineering, Universitas Ahmad Dahlan, Jl Jend. Ahmad Yani (Ringroad Selatan), Tamanan, Banguntapan, Bantul, Yogyakarta, 55166 Yogyakarta, Indonesia

² Department of Chemical Engineering, Universitas Gadjah Mada, Jl Grafika 2, 55281 Yogyakarta, Indonesia

³Department of Chemical Engineering, Indian Institute of Technology Delhi, New Delhi 110016, India

*Corresponding author: sitijamilatun@che.uad.ac.id

Abstract. Bio-oil from microalgae pyrolysis has excellent potential to be developed as a renewable, sustainable, and environmentally friendly energy fuel. Using pyrolysis technology to use the solid waste from microalgae extraction of *spirulina platensis* as an energy source is a solution for pollution due to biomass extraction. The solid residue is known as *Spirulina Platensis* Residue (SPR). SPR pyrolysis will produce liquid fuel (bio-oil), gas, and biochar. This paper discusses the study of the pyrolysis kinetics of SPR with Thermogravimetric analysis (TGA) by flowing nitrogen, the settlement method using *Kissinger - Akahira - Sunose (KAS) and Flynn - Wall - Ozawa (FWO)*. The samples were heated at a temperature ranging from 30°C to 1000°C with three different heating levels, namely 10, 30, and 50°C /min yang injected 20 mL/min Nitrogen (N₂). The results obtained from the thermal decomposition process show three main stages, namely dehydration, active and passive pyrolysis. The activation energy (*Ea*) and the pre-exponential factor (*A*) obtained by the KAS method were around 42.241 kJ/mol, 51.290 kJ/mol, 54.556 kJ/mol, and 61.604 kJ/mol with conversion of 0.2%, 0.3%, 0.4%, while the estimation of activation energy from FWO 48.963 kJ/mol, 58.107 kJ/mol, 61.498 kJ/mol, and 68.457 kJ/mol with conversion of 0.2%, 0.3%, 0.4%, and 0.5% respectively. the kinetic parameter can be described by using this method. The experimental results show that the kinetic parameters obtained from the two methods are slightly different. However, the KAS and FWO methods are quite efficient in explaining the mechanism of the degradation reaction.

1. Introduction

Recently, renewable energy has been one of the interactive issues in Indonesia for discussion in-depth and development because Indonesia has a substantial potential renewable energy source, sustainable energy, and low carbon emission [1]. One type of biomass as an energy source is microalgae which attract attention and have several advantages, including high yield per area, 15 times higher than palm oil, increased efficiency in absorbing, no competition with agriculture and food. In addition, microalgae cultivation can use photo-bioreactor and open water (sea and pond)[2].

There are three main microalgae components: proteins, carbohydrates, and natural oil (lipids). Microalgae can be converted using pyrolysis to produce bio-fuel about 40% at a temperature ranging from 300°C - 500°C [3]. Pyrolysis is a thermochemical process in which biomass decomposes without



Content from this work may be used under the terms of the [Creative Commons Attribution 3.0 licence](https://creativecommons.org/licenses/by/3.0/). Any further distribution of this work must maintain attribution to the author(s) and the title of the work, journal citation and DOI.

oxygen. Next, producing condensable gas in the form of liquid fuel, non-condensable gas, and bio-char as a solid product [4], [5]. Fuel combustion engines can use fuel in liquids and gaseous biofuels with high energy content [6], [7].

An important factor in pyrolysis is the kinetic reaction process where this process is a reaction process which involves reaction time, mass decomposition, and activation energy. [8]. Analysis of reaction kinetics in pyrolysis can be understood in depth using thermogravimetric analysis (TGA)[9]. According to Mishra et al. [10], the TGA method for kinetics study on pyrolysis has high-precision methods. It provides quantitative methods for the examination process and estimation of an effective kinetic parameter. In addition, there are three important procedures to investigate the kinetics and thermal decomposition characteristics of biomass. They are including thermal gravimetric (TG)[11], differential thermal analysis (DTA)[12], and differential thermal gravimetric (DTG) [13].

Next, there are some methods to analyze the kinetic reaction: Model-fitting and model-free methods from isothermal and non-isothermal used in some previous research [14]. According to [15], the fitting model uses several kinetic models for processing TGA data, where the model that provides the best linearization of the TGA data is selected. The model-fitting requires only one TGA data curve for one heating rate. Generally, the model-fitting method is visible to identify in more than one model in the same data with a high fit. However, this makes it challenging to select the best kinetic model. Examples of non-isothermal solid fitting kinetic models are the differential method [16], Freeman-Carroll [17], and Coats-Redfern [18].

Another method to determine decomposition thermal is a model-free method [19]. This method used several data curves at different heating rates to obtain kinetic parameters as a conversion function, commonly called iso-conversion, can be obtained from the calculation. The reaction model used is the same for each conversion with different heating rates. The method for determining these kinetic parameters is quite simple, but the same sample mass and inert gas streams at different heating rates can only carry out [3]. Examples of model-free iso conversion methods are *Flynn-Wall-Ozawa (FWO)*[20], *Kissinger-Akahira-Sunose (KAS)*[21], *Vyazovkin*, *Vyazovkin AIC*, *Friedman*, and *Starink* methods. On the other hand, the Kissinger model is one of the independent models but is not an iso conversion method because the kinetic parameters are assumed to be constant.

The mechanism of the solid-state process, which is a multi-step process with different rates, is complex enough to be approximated by a simple kinetic model [21-22]. This article aims to study the pyrolysis kinetics of *spirulina platensis residue* (SPR). The process mechanism, an iso-conversion method, and the kinetic phenomena in solid-state processes are described in this paper. This method allows the estimation of the kinetic parameters without assuming a reaction model. The effect of temperature and conversion in the thermal decomposition was used in this method as the basic idea. *Kissinger-Akahira-Sunose (KAS)* and *Flynn-Wall-Ozawa (FWO)* as two methods were proposed in this research to determine the kinetic parameters of SPR pyrolysis.

Recently, the thermal degradation of lignocellulosic biomass was widely used to determine the kinetic reaction. The field of biomass such as sewage sludge [23], flax stems [13], [24], waste sawdust [25], and poplar wood [26] conducted the previous research. However, there are few studies related to determining the pyrolysis kinetics of low-lipid microalgae. Therefore, this paper aims to determine the thermal degradation of SPR microalgae with TGA, DTA, and DTG through a free-model approach. The expected result is to help design and improve thermochemical conversion systems for low-lipid microalgae.

2. Materials and Method

2.1. Materials

Spirulina platensis (SPR) residue is a solid residue obtained from *Spirulina platensis* (SP) extraction with methanol as solvent. SPR was analyzed to calorific value at the Laboratory of Food and Agricultural Products, Department of Agricultural Technology. The Laboratory of Food and Nutrition, Center for Inter-University (PAU) UGM conducted the proximate analysis. At the same time, the ultimate analysis was carried out at the Testing Laboratory, Tekmira Research and Development Center, Bandung. The Characteristics of SPR are shown in table 1.

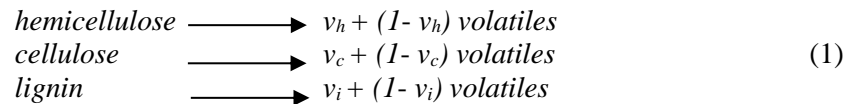
Table 1. Characteristics of SPR

Component	SPR
Elemental analysis (wt%)	
Carbon	41.36
Hydrogen	6.60
Nitrogen	7.17
Oxygen	35.33
Higher heating value (MJ/kg)	18.21
Composition (dry-ash-free, wt%)	
Protein	49.60
Lipid	0.01
Carbohydrate	25.60

2.2. Methods

2.2.1. Experiments. Thermal decomposition was tested using TG–DTA (Perkin Elmer Pyris Diamond) at the Academy of Skin Technology, Yogyakarta (Yogyakarta ATK Polytechnic). The SPR as a raw material for each experiment was 4–8 mg. The temperature ranges from 30 to 1000°C together with heating rates of 10, 30, and 50 °C/min. 20 mL/min of nitrogen was injected to maintain oxygen-free pyrolysis conditions with a high-purity nitrogen stream carried out the heating rate.

2.2.2. Kinetic Modeling. The one-step global model assumes that the devolatilization phenomenon takes place as a single reaction. This model was introduced by [27], [28]. Heating rate was used to find TG curve. Three components of biomass (hemicellulose, lignin, and cellulose) was established as equation 1.



Where v represents the char yield of the reaction while (h, c, i) denotes hemicellulose, cellulose, and lignin, in general, decomposition reaction in this model is produced a volatile substance and char.

The sample was pyrolyzed with a non-isothermal thermogravimetric analysis (TGA), and the change in weight of the sample was recorded. The conversion rate for time or degradation, dX/s , depends on the reaction rate constant, which is affected by temperature, $k(T)$, and the conversion, $f(X)$. Equation 2 expressed the detail of TGA as:

$$\frac{dX}{dt} = k(T)f(X) \quad (2)$$

Where X is the conversion, t is the time in minutes, T is the temperature in Kelvin. The rate constant for the reaction represented as k follows the Arrhenius equation:

$$k(T) = Ae^{(-E_a/RT)} \quad (3)$$

Where E_a is the activation energy of the reaction (kJ mol^{-1}), T is the absolute temperature (K), R is the gas constant ($8,314 \text{ J/Kmol}^{-1}$), and A is the pre-exponential factor (min^{-1}). If the conversion (X) is expressed by [24], then the conversion rate from solid-state to volatile product ($d\alpha/dt$) can be written by the following equation:

$$\frac{d\alpha}{dt} = k(T)f(\alpha) \quad (4)$$

Where α , t , $k(T)$, and $f(\alpha)$ are symbols of conversion rate, time, the reaction rate constant, and conversion, respectively. Calculating the mass at the initial time can also use α and $k(T)$ as follows:

$$\alpha = \frac{m_i - m_a}{m_i - m_f} \quad (5)$$

where:

- m_a is the weight of SPR at time t ,
- m_i is the initial weight of SPR, and
- m_f is the final weight of SPR at the end of the reaction.

The combination of the two equations (4) and (5) gives the expression of the fundamental in equation (6) analytical method for calculating the kinetic parameters, based on the TGA results.

$$\frac{d\alpha}{dt} = A \cdot f(\alpha) \cdot e^{-E_a/RT} \quad (6)$$

The expression function $f(\alpha)$ is used to describe a first-order reaction for the solid-state. Hence many authors limit the mathematical function $f(\alpha)$ to the following expression:

$$f(\alpha) = (1 - \alpha)^n \quad (7)$$

Where n presents the order of the reaction. From the equations (6) and (7) becoming equation (8) states the reaction rate in the form:

$$\frac{d\alpha}{dt} = A \cdot (1 - \alpha)^n e^{-E_a/RT} \quad (8)$$

For the heating, the rate can express it as

$$\beta = \frac{d\alpha}{dT} = \frac{d\alpha}{dt} \frac{dt}{dT} \quad (9)$$

Where $d\alpha/dT$ is the non-isothermal reaction rate and substitution of equations (8) and (9), this produces the following equation:

$$\frac{d\alpha}{dt} = \frac{A}{\beta} (1 - \alpha)^n e^{-E_a/RT} \quad (10)$$

Equation (10) is reduced to a linear equation; furthermore, the kinetic parameters are evaluated from the plot of the y-axis versus the x-axis that is the fundamental equation to determine the thermal degradation kinetic methods using iso-conversion methods [29]. In this study, two general iso-conversion methods are performed by *Kissinger-Akahira-Sunose* (KAS) and *Flynn-Wall-Ozawa* (FWO) [26]. According to [30], the KAS and FWO method can be selected and applied to determine TG/DTG data. The advantage of KAS and FWO methods is that the calculated activation energy (E_a) is allowed without any prior knowledge of the analytical form of the conversion function (f_a) [31]. This method also can provide a capability to describe the kinetic mechanics of pyrolysis [32].

2.3. Model-free methods

2.3.1. Kissinger – Akahira – Sunose (KAS). Kissinger-Akahira-Sunose (KAS) method is an iso-conversion method to obtain the kinetics of the solid-state reaction without knowing the reaction mechanism. This method was introduced by [33] that variation of peak temperature with heating rate can be derived from the kinetic of reaction in a differential thermal. In this paper, the equation (10) can be derived to the equation (11) by using KAS methods as follows:

$$\ln\left(\frac{\beta_i}{T_{ai}^2}\right) = \ln\left(\frac{A_{\alpha} R}{E_{\alpha} g_{\alpha}}\right) - \frac{E_{\alpha}}{RT_{ai}} \quad (11)$$

Where i is the heating rate, $T_{\alpha i}^2$ is the temperature for each predefined conversion at different heating rates, E_{α} is the activation energy for each conversion, A_{α} is the pre-exponential factor for each conversion, g_{α} as the integral of $f(\alpha)$. The slope of the graph ($-E_{\alpha}/RT$) is used to calculate the activation energy. Meanwhile, the intercept plot $\ln(\beta_i/T_{\alpha i})$ versus $1000/T_{\alpha i}$ shows a pre-exponential factor.

2.3.2 Flynn – Wall – Ozawa Method. The FWO method was introduced by [34], [35] which it makes possible to obtain the activation energy (E_{α}) of the logarithm of the heating rate, $\ln\beta_i$, versus $1052/T_{\alpha i}$, which represents a linear relationship with specific conversion values at different heating rates. *Flynn-Wall-Ozawa* (FWO) method was another iso- conversion method that can be expressed as in equation 12 as follows:

$$\ln(\beta_i) = \ln\left(\frac{A_{\alpha}E_{\alpha}}{Rg(\alpha)}\right) - 5.331 - 1.052 \frac{E_{\alpha}}{RT_{\alpha i}} \quad (12)$$

Where $g(\alpha)$ is constant at the given conversion value, the subscripts i and α show the offered heating rate and conversion value, respectively. The activation energy E_{α} is calculated from the slope of $1.052E_{\alpha}/R$. Calculating the slope ($1.052E_{\alpha}/R$) and the intercept plot (β_i) versus $1000/T_{\alpha i}$ estimated the slope activation energy and pre-exponential factor.

3. Result and Discussion

3.1. Thermogravimetric Analysis

The thermal decomposition of *Spirulina platensis* residue (SPR) can be determined by thermogravimetric analysis shown by the DTA, TG, and DTG curves. The DTA curve is used to describe the temperature difference between a substance and a thermally inert reference material that is measured as a function of the temperature (T). The TG curve is used to describe the thermal analysis, and the DTG curve is used to describe the weight loss or increase at heating rate. The experiment was carried out at a temperature ranging from 30°C to 1000°C with a heating rate of 10, 30, dan 50 °C/min, respectively, flowed 20 mL/minute nitrogen (N_2). The profile of sample mass (TG curve) can be expressed by the thermo-gravimetric analysis directly. The shape of derivative mass losses (DTG) can be defined by $d(m/m_o)/dT$. Figures 1 and 2 can describe the TG-DTG profile.

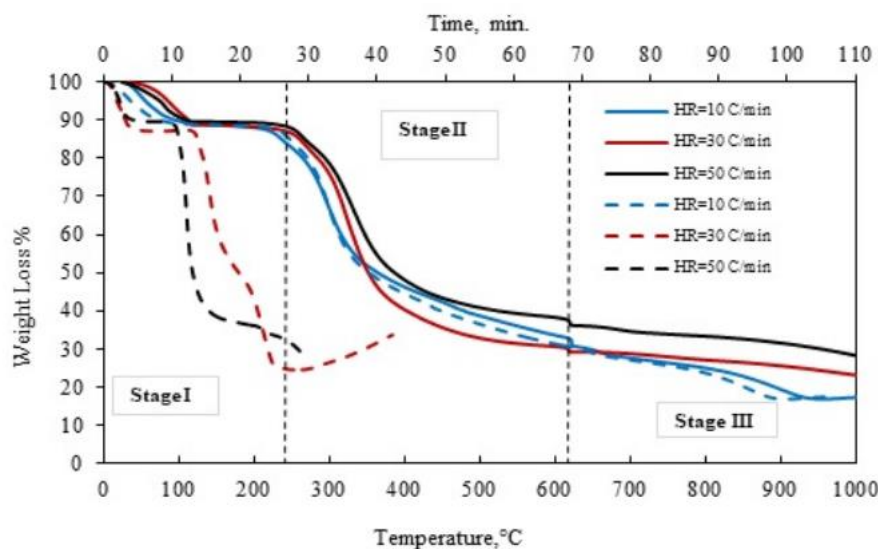


Figure 1. TG of weight loss curves of spirulina platensis residue at three heating rates with three stages: dehydration, active and passive pyrolysis

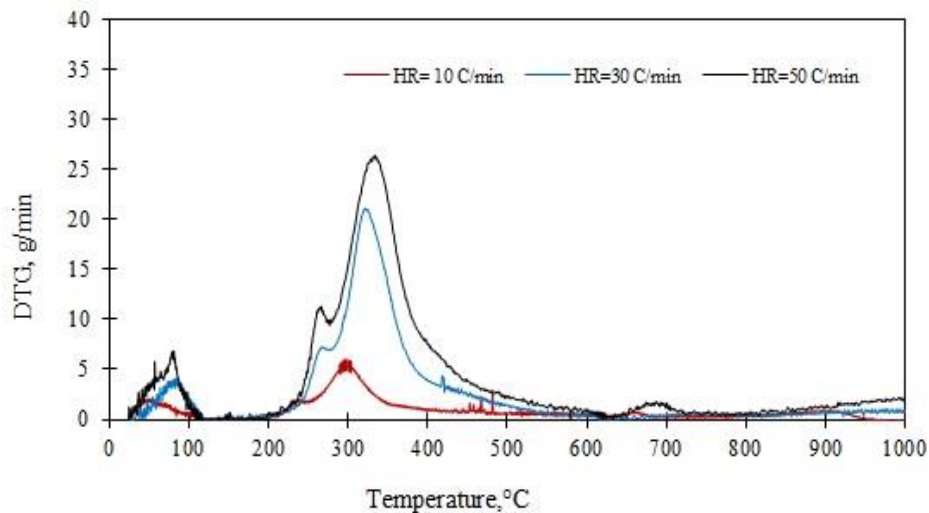


Figure 2. DTG of a spirulina platensis residue at different heating rates.

Figure 1 Indicated that the thermal decomposition process of SPR was divided into three stages: water dehydration, active pyrolysis, and passive pyrolysis. The effect of temperature on pyrolysis is proportional to the process of mass decomposition at SPR which the pyrolysis temperature increases while the mass weight decreases slightly. The pyrolysis temperature increases with increasing heating rate, but the final temperature was not affected. The detail of thermal decomposition is described in table 2.

Table 2. Thermal decomposition of SPR

Thermal decomposition	Heating rate (°C/min)		
	10	30	50
Stage I (water dehydration)	30°C - 220°C	30°C - 240°C	30°C - 260°C
Stage II (active pyrolysis)	221°C - 615°C	241°C - 585°C	261°C - 600°C
Stage III (passive pyrolysis)	616°C - 1000°C	586°C - 1000°C	601°C - 1000°C

The water dehydration process releases water content, adsorbed water on the SPR sample, and evaporates the light volatile components. Weight loss in stage I is around 11-15%. Weight loss in the active pyrolysis process is about 55-60%. In the active pyrolysis process, most cellulose and hemicellulose are decomposed to produce chemical compounds such as benzene, toluene, phenol alkenes, and alkanes, among other compounds. The passive pyrolysis process, commonly called gasification, occurs when lignin is decomposed. The nature of lignin is relatively stable to heat so that the decomposed mass is quite small and the weight loss is insignificant. The weight loss curve (TG) in figure 1. shows the mass loss with the temperature at different heating rates on the SPR. Thermal decomposition in this study was relevant with some literature survey that summary is listed in table 3, which includes the TGA technique in the previous research and pyrolysis behavior into three stages.

Table 3. Investigations on pyrolysis behavior using thermogravimetric Analysis from the previous study

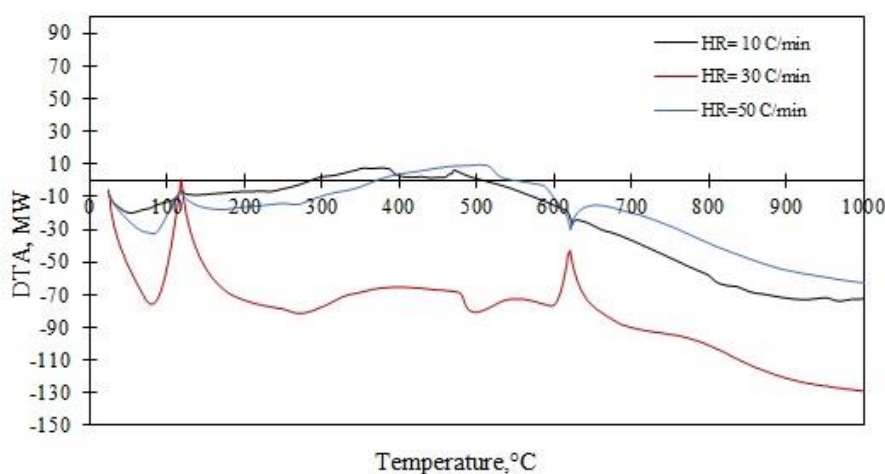
Heating rate (°C/min)	Temp operation (°C)	Mass loss temperature range (°C)						Ref
		Stage 1	Mass loss of stage 1	Stage 2	Mass loss of stage 2	Stage 3	Mass loss of stage 3	
10, 40, 70, and 100	0-1000	25-200	10%	200-600	41.5%	>600	Lower mass loss	[36]
5, 10, and 20	0-1000	25-200	Moisture loss	200-600	-	>600	-	[37]
10, 20, and 30	100-1000	<150	0.87%	150-584	35.49%	584-800	5.07%	[38]
5, 10, 20, and 30	25-900	25-200	Moisture loss	200-500	55%	500-600	20%	[39]
10	25-900	150-300	22.5%	200-450	41.7%	450-600	5.7%	[40]

The effect of derivative thermogravimetric (DTG) on heating rate can be seen in figure 2. DTG curve indicates that when the heating rate increases, the DTG value also increases, and the DTG curve changes based on the higher temperature range. In this process, the active and passive pyrolysis region is also increasing. Different heating rates in this experiment was 10°C/min, 30°C/min, and 50°C/min which mass decomposition in heating rate 10°C/min begins on a reasonably low curve and at a temperature of 300°C. In contrast, the heating rate of 30°C/min and 50°C/min occurs in the temperature ranging from 350°C to 600°C. Then, above a temperature of about 700°C, the process of mass decomposition proceeds slowly. The TG and DTG curves with variations in heating rate tend to shift towards higher temperatures. The starting point and endpoint of the active pyrolysis region are located at higher temperatures for higher heating rates. The range of active pyrolysis decomposition rates is extensive for higher heating rates. The higher the heating rate, the maximum decomposition rate is located at a higher temperature and has a higher value. This phenomenon indicates that there is a limit to heat transfer. An immediate amount of energy is required for the system. It takes a longer reaction time to reach a temperature equivalent to the furnace temperature when low heating rate. The reaction time is shorter at a higher heating rate, so the sample requires a higher temperature to decompose. These results were consistent with the prevision research in the field of microalgae. The detail of the comparison from previous research is described in table 4.

Table 4. Comparison of the thermal decomposition of microalgae

Microalgae Species	Experiment result			Heating Rate	Ref
	Stage I	Stage II	Stage III		
Chlorella Vulgaris	Temperature ranging from 25°C to 150°C. in this stage, water and light volatile compound are lost	Temperature ranging from 150-450°C. most of the organic species are decomposed in this stage	From 460-600°C. in this stage, there are very slight weight losses, and carbonaceous reduction are decomposed	heating rate of 10, 20, and 40°C/min.	[41]
Spirulina Sp	Starting at 50-200°C. the first stage is dehydration which moisture remove from the sample	Starting at 200-600°C. in the second stage, the weight loss is approximately 60%	Starting at 600-900°C, the weight loss is lost slowly.	the heating rate of 10 °C/min and temperature ranging from 50-600°C	[42]
Chlorella Vulgaris	Starting at 0-150 °C	Starting at 150-450°C, in this stage, the thermal degradation of carbohydrate, protein, and lipid was lost	Starting at higher than 540°C. the thermal degradation was decayed slightly	heating rate 10 °C/min and 20 °C/min	[43]
This study	Process dehydration occurs in this stage, with temperature ranging from 30 to 220 °C	Starting at 221-615°C active pyrolysis occurs in this stage	Starting at 616-1000°C Passive pyrolysis occurs in this stage	the heating rate of 10 °C/min, 30 °C/min, and 50 °C/min	

Differential thermal analysis (DTA) of SPR can be seen in figure 3. During the TGA experiment, constant heating rate measures the temperature difference between the heating temperature of SPR and the references material. The peak of the DTA curve represents the thermal condition which a positive peak value describes an endothermic process while a negative value indicates the exothermic process.

**Figure 3.** Differential thermal analysis (DTA) of SPR

3.2 Kinetic analysis based on the KAS and FWO

Kinetic analysis based on the KAS and FWO was used to calculate the kinetic parameters from a thermogravimetric study using the model-free method. The activation energy (E_a) and the pre-exponential factor (A) were obtained using the *Kissinger-Akahira-Sunose* (KAS) and *Flynn-Wall-Ozawa* (FWO) methods. The KAS method uses equation (11) to determine the activation energy and pre-exponential factor. At the same time, the FWO method uses equation (12) to determine the activation energy and pre-exponential factor. The plot of regression shown from $\ln(\beta/T^2m)$ versus $1000/T_m K^{-1}$ that illustrated in figure 4. The regression and quadratic equations of the correlation coefficient (R^2) are also presented. The activation energy (E_a) and the pre-exponential factor (A) are derived from the slope and cross of the plotting regression line, respectively. The results obtained from the KAS method are provided in table 3; the average activation energy (E_a) value and the pre-exponential factor of KAS methods are 52.423 kJ/mol and 1.363×10^4 . The experiment was used the same value of α from range 0.20 to 0.50. The heating rate in this calculation was followed by figure 1, in which β indicated from 10, 30, and 50°C/min.

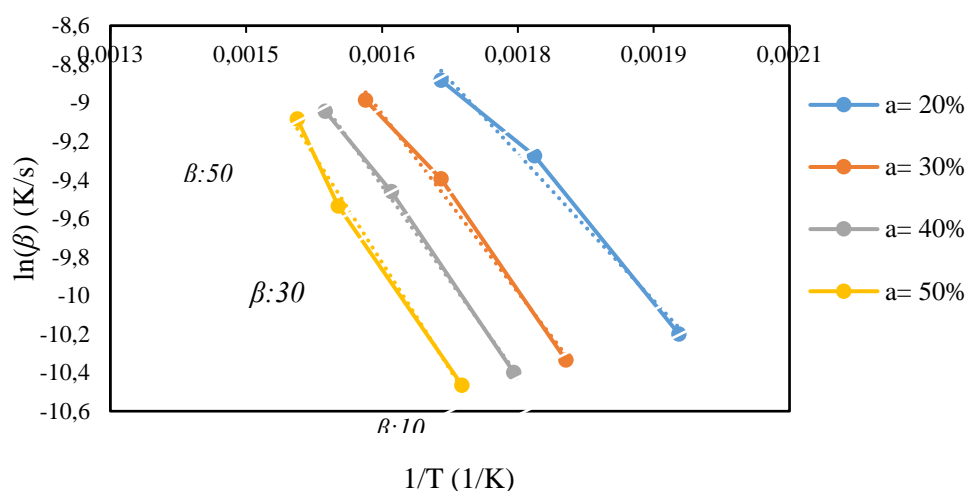


Figure 4. KAS Method of kinetic analysis of SPR

Figure 4 shows the change in conversion with the sample temperature at different heating rates in determining the kinetic parameters. The results of the activation energy value calculation, pre-exponential, can be seen in table 3, which all curves at different heating rates, and we find the appropriate temperature. Plot FWO was described in $\ln(\beta i)$ versus $1000/T_{ai} K^{-1}$ other conversion value shown in figure 5. The activation energies are obtained from the slope and pre-exponential factor of the regression line intercepts and are given in table 5—the calculated square of the correlation coefficient, R^2 . The average activation energy (E_a) value and pre-exponential (A) of FWO methods are 59.257 kJ/mol and 8.206×10^4 .

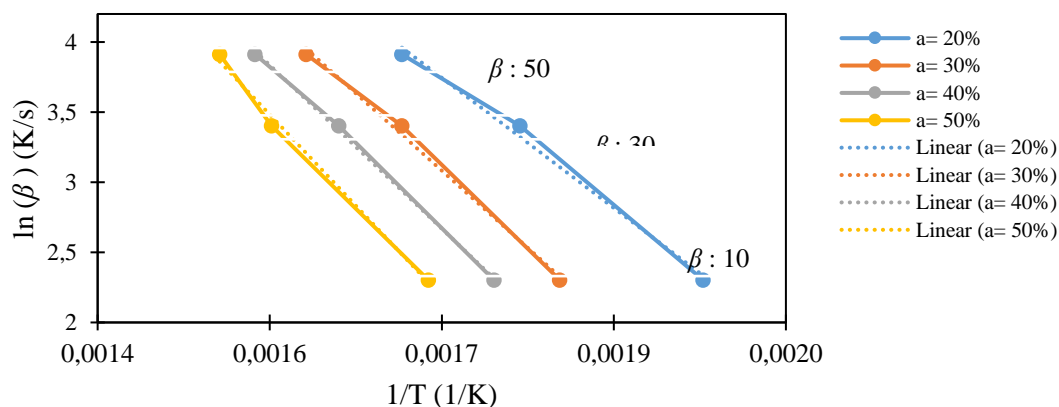


Figure 5. FWO method of kinetic analysis of SPR

Thermogravimetric analysis is a common technique used to evaluate the thermal decomposition of biomass. In addition, iso-conversion methods such as KAS, FWO, and Kissinger are widely used to determine the kinetic parameters. In this study, KAS and FWO were used to determine the SPR reaction kinetics.

Table 5. The activation energy of SPR obtained by KAS and FWO method

α (x/%)	KAS Method			FWO Methods		
	Activation Energy, E_a (kJ/mol)	A (min^{-1})	Coefficient of Determinati on, R^2	Activation Energy, E_a (kJ/mol)	A (min^{-1})	Coefficient of Determinat ion, R^2
0.20	42.241	0.781×10^3	0.9886	48.963	7.134×10^3	0.9929
0.30	51.290	4.963×10^3	0.9931	58.107	3.536×10^4	0.9955
0.40	54.556	9.755×10^3	0.9978	61.498	6.564×10^4	0.9986
0.50	61.604	3.902×10^4	0.9927	68.457	2.201×10^5	0.9944
Average	52.423	1.363×10^4		59.257	8.206×10^4	

The appearance of activation energy by using KAS and FWO methods can be seen in figure 6. From the calculation, the energy activation from KAS and FWO is not the same for all conversions that can observe. It suggests the existence of a complex multi-step mechanism that occurs in the solid state. This mechanism shows that the reaction mechanism is not the same in the overall decomposition process, and the activation energy depends on the conversion. The estimation of activation energy from KAS method is around 42.241 kJ/mol, 51.290 kJ/mol, 54.556 kJ/mol, and 61.604 kJ/mol with conversion of 0.2%, 0.3%, 0.4%, and 0.5% respectively. While the estimation of activation energy from FWO 48.963 kJ/mol, 58.107 kJ/mol, 61.498 kJ/mol, and 68.457 kJ/mol with conversion of 0.2%, 0.3%, 0.4%, and 0.5% respectively. These results are indicated that activation energy from FWO is more than the activation energy of the KAS method. The clear correlation between conversion and activation energy can be seen in figure 6.

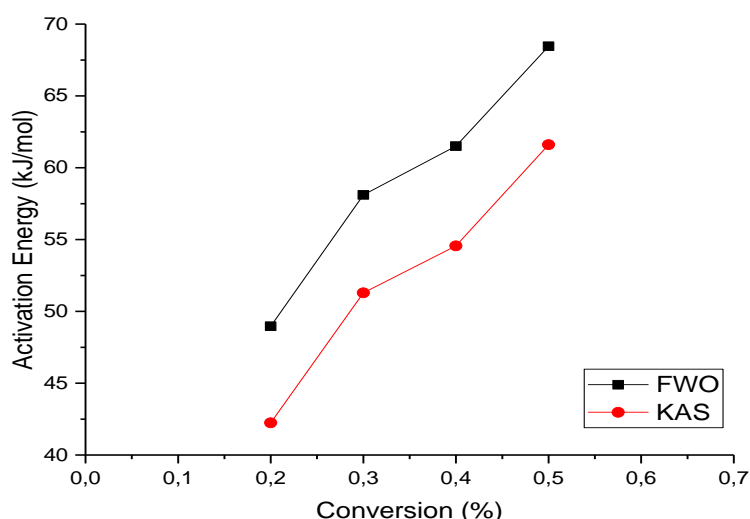


Figure 6. The activation energy is a function of conversion.

The use of KAS and FWO methods were justified the ICTAC committee's recommendation for a model-free method and affected by the use of catalyst. The term of its dependability validated the kind of biomass the experiment in this study was without these methods. Based on table 6 obtained, the average activation energy in this study is relevant to several kinds of literature. KAS and FWO methods

were proven and able to interpretation the kinetic reaction of biomass. The difference of activation in this study with the previous research was a catalyst.

Table 6. the comparison of kinetic methods and activation energy from the previous study

Biomass types	Methods	Activation energy (kJ/mol)	references
Banana leaves	KAS, FWO, Starink, and Friedman	79.36, 84.02, 92.12, and 73.89	[44]
Sugar leaves	FWO, KAS, and Starink	226.97, 226.75, and 226.94	[45]
Coconut shell	FWO and KAS	99.2 and 94.7	[46]
Chlorella	KAS and FWO	148.75 and 150.99	[47]
Vulgaris with catalyst			
C. Vulgaris	KAS and FWO	131.228 and 142.678	[41]

4. Conclusion

Kinetic studies on *Spirulina Platensis* Residue (SPR) in this study are presented in DTA, TG, and DTG curves to determine the mass decomposition of the reaction. In addition, the calculation of kinetic analysis to determine the response kinetics parameters from the results of the thermogravimetric study uses the model-free method. The activation energy (E_a) and pre-exponential factor (A) were obtained by the *Kissinger-Akahira-Sunose* (KAS) and *Flynn-Wall-Ozawa* (FWO) methods. The process of mass decomposition in SPR occurs in 3 areas: dehydration, active pyrolysis, and passive pyrolysis. The effect of temperature on pyrolysis is proportional to the process of mass decomposition at SPR. The higher the pyrolysis temperature, the higher the weight loss. The water dehydration process occurs at a temperature of 30°C-240°C. Active pyrolysis process from 240-610°C, and passive pyrolysis process from 610 - 1000°C called gasification where lignin is decomposed. The plot of KAS shown from $\ln(\beta/T^2m)$ versus $1000/T_mK^{-1}$. At the same time, Plot FWO is shown as $\ln(\beta i)$ versus $1000/TaK^{-1}$ for different conversion values. The average activation energy (E_a) value dan pre-exponential (A) of KAS methods are 52.423 kJ/mol and 1.363×10^4 .

In comparison, the average activation energy (E_a) value dan pre-exponential (A) of FWO methods are 59.257 kJ/mol and 8.206×10^4 . The appearance of activation energy by using KAS and FWO methods is not similar. The FWO and KAS methods of activation energy and pre-exponential factors show the mechanism of complex reactions during the pyrolysis process.

5. Reference

- [1] Jacobson K, Maheria K C, and Dalai A K 2013 *Renew. Sustain. Energy Rev.* **23** 91–106
- [2] Priyadarshani I and Rath B 2012 *J. Algal Biomass Utiln.* **3(4)** 89–100
- [3] Jamilatun S, Mufandi I, Evitasari R T, and Budiman A 2020 *Int. J. Renew. Energy Res.* **10(2)** 678–686
- [4] Bridgwater A 2013 Fast pyrolysis of biomass for the production of liquids in *Woodhead Publishing Series in Energy, Biomass Combustion Science, Technology and Engineering* Woodhead Publishing
- [5] Treedet W, Suntivarakorn R, Mufandi I, and Singbua P 2020 *Int. Energy J.* **20(2)** 155–168
- [6] Xu Y, Hu Y, Peng Y, Yao L, Dong Y, Yang B, Song R 2020 *Bioresour. Technol.* **300(October 2019)** 122665
- [7] Mufandi I, Treedet W, Singbua P, and Suntivarakorn R 2020 *KKU Res. J.* **20(December)** 94–107
- [8] Chen R, Zhang D, Xu X, and Yuan Y, 2021 *Fuel* **295**
- [9] Saeed S, Ashour I, Sherif H, and Ali M R O 2020 *Egypt. J. Chem.* **63(2)** 683–702
- [10] Mishra G, Kumar J, and Bhaskar T 2015 *Bioresour. Technol.* **182** 282–288
- [11] Singh S, Patil T, Tekade S P, Gawande M B, and Sawarkar A N 2021 *Sci. Total Environ.* **783** 147004
- [12] Wen Y, Wang S, Mu W, Yang W, and Jönsson P G 2020 *Fuel* **277(December 2019)** 118173

- [13] Wang X, Hu M, Hu W, Chen Z, Liu S, Hu Z, and Xiao B 2016 *Bioresour. Technol.* **219** 510–520
- [14] Soria-Verdugo A, Morgano M T, Mätzing H, Goos E, Leibold H, Merz D, Riedel U, and Stapf D 2020 *Energy Convers. Manag.* **212(April)** 112818
- [15] Mandapati R N and Ghodke P K 2021 *Fuel* **303(June)** 121285
- [16] Pan L, Dai F, Li G, and Liu S 2015 *Energy*. **86** 749–757
- [17] Criado J M, Dollimore D, and Heal G R 1982 *Thermochim. Acta* **54(1–2)** 159–165
- [18] Mian I, Li X, Jian Y, Dacres O D, Zhong M, Liu J, Ma F, and Rahman N 2019 *Bioresour. Technol.* **294(August)** 122099
- [19] Liu H, Chen B, and Wang C 2020 *Fuel Process. Technol.* **208(June)** 106509
- [20] Yang H, Ji G, Clough P T, Xu X, and Zhao M 2019 *Fuel Process. Technol.* **195(May)** 106145
- [21] Lim A C R, Chin B L F, Jawad Z A, and Hii K L 2016 *Procedia Eng.* **148** 1247–1251
- [22] Lopes F C R and Tannous K 2020 *Thermochim. Acta*, **691(April)** 178714
- [23] Liu H, Xu G, and Li G 2021 *Process Saf. Environ. Prot.* **149** 48–55
- [24] Ding Y, Ezekoye O A, Lu S, Wang C, and Zhou R 2017 *Energy Convers. Manag.* **132** 102–109
- [25] Mishra R K and Mohanty K 2018 *Bioresour. Technol.* **251(October 2017)** 63–74
- [26] Slopiecka K, Bartocci P, and Fantozzi F 2012 *Appl. Energy* **97** 491–497
- [27] Ding Y, Ezekoye O A, Zhang J, Wang C, and Lu S 2018 *Fuel* **232(May)** 147–153
- [28] Ding Y, Wang C, Chaos M, Chen R, and Lu S 2016 *Bioresour. Technol.* **200** 658–665
- [29] Islam M A, Auta M, Kabir G, and Hameed B H 2016 *Bioresour. Technol.*, **200(October 2017)** 335–341
- [30] Rahib Y, Sarh B, Bostyn S, Bonnamy S, Boushaki T, and Chaoufi J 2020 *Mater. Today Proc.* **24** 11–16
- [31] Mothé C G and De Miranda I C 2013 *J. Therm. Anal. Calorim.* **113(2)** 497–505
- [32] Rego F, Dias A P S, Casquilho M, Rosa F C, and Rodrigues A 2020 *Energy* **207** 118191
- [33] Kissinger H E 1956 *Cardiovasc. Probl. Emerg. Med. A Discuss. Rev.* **57(4)** 123–137
- [34] Smith I T 1964 *Naturae Publ. Gr.* **201** 69
- [35] Ozawa T 1965 *Bull. Chem. Soc. Jpn.* **38(11)** 1881–1886
- [36] Kan T, Strezov V, and Evans T 2016 *Energy and Fuels* **30(3)** 1564–1570
- [37] Naqvi S R, Tariq R, Shahbaz M, Naqvi M, Aslam M, Khan Z, Mackey H, McKay G, and Al-Ansari T 2021 *Comput. Chem. Eng.* **150** 107325
- [38] Lin Y, Liao Y, Yu Z, Fang S, Lin Y, Fan Y, Peng X, and Ma X 2016 *Energy Convers. Manag.*, **118** 345–352
- [39] Im H and Kim C G 2017 *J. Mater. Cycles Waste Manag.* **19(3)** 1044–1051
- [40] Cao J P, Shi P, Zhao X Y, Wei X Y, and Takarada T 2014 *Fuel Process. Technol.* **123** 34–40
- [41] Azizi K, Moraveji M K, and Najafabadi H A 2017 *Bioresour. Technol.* **243** 481–491
- [42] Chaiwong K, Kiatsiriroat T, Vorayos N, and Thararax C 2013 *Biomass and Bioenergy* **56** 600–606
- [43] Bach Q V and Chen W H 2017 *Energy Convers. Manag.* **131** 109–116
- [44] Singh R K, Pandey D, Patil T, and Sawarkar A N 2020 *Bioresour. Technol.* **310(April)** 123464
- [45] Kumar M, Sabharwal S, Mishra P K, and Upadhyay S N 2019 *Bioresour. Technol.* **279(January)** 262–270
- [46] Ali I, Bahaitham H, and Naibulharam R 2017 *Bioresour. Technol.* **235** 1–11
- [47] Bong J T, Loy A C M, Chin B L F, Lam M K, Tang D K H, Lim H Y, Chai Y H, and Yusup S 2020 *Energy* **207** 118289

Acknowledgments

The author would like to thank the research funding assistance through the Internal Research Fund Scheme through the Lembaga Penelitian dan Pengabdian Masyarakat Universitas Ahmad Dahlan Yogyakarta.